Simulation study of a high-intensity linear accelerator operated at longitudinal phase advances above 90°

A. Rubin and L. Groening

GSI Helmholtzzentrum für Schwerionenforschung GmbH, Planckstraße 1, D-64291 Darmstadt, Germany

I. Hofmann*

Technische Universität Darmstadt, Schlossgartenstraße 8, 64289 Darmstadt, Germany

(Received 5 October 2020; accepted 14 December 2020; published 30 December 2020)

High intensity beams may suffer from serious beam quality degradation if the focusing scheme allows for occurrence of resonances or instabilities. For transverse focusing a commonly accepted and respected lattice design rule is to choose the phase advance per structure period below the 90° resonant stop band, which was implicitly applied to the longitudinal phase advance the same way. A recent study pointed out that for lattice structures with more than one rf gap per period the 90° restriction needs not to be applied the same way to the longitudinal focusing as to the transverse one [I. Hofmann and Oliver Boine-Frankenheim, Phys. Rev. Lett. **118**, 114803 (2017)], thus offering more design flexibility. The present paper is motivated by an interest to accelerate intense proton beams above longitudinal 90° in the new poststripper drift tube linac of the GSI universal linear accelerator by using the rf power supplies optimized for the much stiffer heavy ions. We confirm that a strictly periodic prolongation of the first cavity could allow acceleration above longitudinal 90° with only minor beam quality degradation. However, the combination of a high longitudinal phase advance with intercavity sections breaking the periodicity shows that matching challenges—rather than resonances—determine emittance growth. In the present case it is found tolerable for up to three such sections. This confirms the validity of the principle and at the same time its limits under practical conditions.

DOI: 10.1103/PhysRevAccelBeams.23.124202

I. INTRODUCTION

For the design and optimization of linear accelerators at high intensity it is common practice to observe a number of criteria based on space charge controlled beam dynamics, like smooth changes in transverse and longitudinal focusing; good matching between lattice transitions; avoid emittance transfer; and—of interest here—keep the zero current phase advance per cell below 90° in all directions (see, for example, Refs. [1–4]). The two last criteria are resonant processes, which matter even in relatively short sections due to the high level of space charge in high-intensity linacs.

Historically, the transverse 90° stop band was studied first as "transverse envelope instability," and the limit of zero current phase advance $k_{0,t} \leq 90°$ was adopted [5,6]. A significant rms-emittance growth above 90°—without phase space analysis—was evidenced in a transport channel experiment [7].

The existence of the transverse 90° stop band in an rf linac was evidenced experimentally much later in an experiment at the GSI universal linear accelerator (UNILAC) [8]. Detailed measurements clarified that the resonant response was due to a fourth order resonance driven by the periodic—structure modulated—space charge pseudo-octupole. This experiment was supported theoretically and proposed in Ref. [9].

The 90° stop band actually always combines two distinct mechanisms: the fourth order space charge resonance, which sets in immediately, and the second order envelope instability, which grows exponentially from an initial mismatch [10,11]. The relatively short length of 15 structure periods and good initial matching in the UNILAC experiment was understood as the reason why the transverse envelope instability could not be seen [11].

The assumption that $k_{0,t} \leq 90°$ equally applies to the longitudinal plane as $k_{0,z} \leq 90°$—defined over the same focusing lattice structure period—was implicitly adopted in linac design. The justification for this can be seen in the fact that—in a strict sense—3D space charge coupling also imprints the transverse periodicity onto the longitudinal degree of freedom. However, a recent study pointed out that

*Also at GSI Helmholtzzentrum für Schwerionenforschung GmbH, Planckstraße 1, D-64291 Darmstadt, Germany.

in a periodic lattice this longitudinal constraint is unnecessary, if several equally distanced rf gaps exist per lattice structure period, which is normally the case in drift tube linacs or in designs of superconducting linacs employing quadrupoles for focusing [12]. This way the effective longitudinal period is only a fraction of the lattice structure period, and the longitudinal 90° stop band is eliminated. A 3D envelope instability study recently demonstrated that breaking the condition of equal distances is harmful to this elimination [13].

Furthermore, Ref. [12] also showed that in periodic lattices a newly discovered "sum mode" can couple the transverse and longitudinal 90° modes unless the sum criterion $k_{0,z} + k_{0,t} \leq 180°$ is observed (see also Refs. [13–15] on the sum modes). However, for relatively short linacs it can be assumed that this sum criterion has no significant effect.

This paper provides a test bed for this 90° stop band issue in a real machine design including acceleration by using the new poststripper drift tube linac (DTL) layout of the universal linear accelerator (UNILAC) at GSI [16,17]. It comprises four focusing (F) - defocusing (D) periodic lattice sections with a transverse FDDF focusing scheme separated by three intercavity sections.

Our study proceeds in several steps: a short review of the new UNILAC poststripper DTL in Sec. II is followed by Sec. III presenting simulation results for acceleration of protons in the first cavity of the new DTL as well as in an idealized strictly periodic prolongation; in Sec. IV this prolonged structure is interrupted by different numbers of intercavity sections; in Sec. V the real UNILAC poststripper is operated longitudinally at 120° for acceleration of intense proton beams; with conclusions drawn in Sec. VI.

II. THE UNILAC POSTSTRIPPER DTL DESIGN

The present study for proton acceleration is carried out by using the design of the new DTL at GSI optimized for heavy ions, which will be built to meet the requirements of the FAIR project currently under construction [18]. Its main design parameters are listed in Table I. For ion accelerators usually beam currents are stated as electrical (e) currents being the number of ions per second multiplied by their charge number q and the positive unit charge e in Coulomb. For protons and electrons the (e) in the unit of current is omitted as $|q| = 1$. This new Alvarez-type DTL has a length of 57 m and consists of five cavities with 54, 22, 41, 35, and 28 rf cells, respectively. The transverse focusing lattice applies the FDDF scheme [19,20] as depicted in Fig. 1. The quadrupoles inside of drift tubes (DT) are grouped into families of different effective lengths as listed in Table II. Figure 2 shows one of the intercavity sections AI-AIIa, AIIb-AIII, and AIII-AIV having a length of one meter each and consisting of three quadrupoles, one rebuncher, and current and phase probes. The first and the last intercavity quadrupole with effective lengths of 96 mm are placed partially inside the adjacent cavity half DT. The central quadrupole is 134 mm long and the rebuncher is located behind the central quadrupole. The section between AIIa-AIIb consists of a two-gaps rebuncher continuing the periodic lattice from cavity AIIa to AIIb. Accordingly, the DTL is made from five cavities and four periodic lattice sections.

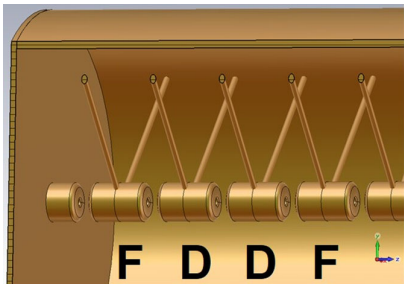

FIG. 1. One complete DTL period comprising four quadrupoles and four rf gaps.

Although the DTL design is optimized for acceleration of $^{238}U^{28+}$ with electrical current of 16.5 emA, it might be requested to deliver protons as well. Straightforward adaption of the longitudinal lattice to protons would imply operation of the rf power sources below their limit of stability. To avoid this the design rf phase is lowered from the nominal −30° by simultaneous increase of the voltage and longitudinal phase advance. Hence, for FAIR the issue of high longitudinal stability at 90° and beyond is of direct practical impact to the achievable beam parameters and to the accessible physics experimental program. Accordingly, the goal of the presented investigations is to benchmark the findings of Ref. [12]: first, to gain insight into beam dynamics along the new poststripper DTL for proton beams with regard to beam stability for different phase

TABLE I. Main parameters of the new poststripper DTL. Its design was used for simulations with 2.0 mA of protons.

Ion A/q	≤8.5
Beam current	1.76 A/q emA
Input beam energy	1.4 MeV/u
Output beam energy	3.3–11.4 MeV/u
Beam pulse length	≤1.0 ms
Beam repetition rate	10 Hz
rf frequency	108.408 MHz

TABLE II. Effective lengths of the DTL quadrupoles.

AI	DT 1–15: 96 mm
	DT 16–36: 113 mm
	DT 37–54: 134 mm
AIIa	155 mm
AIIb	193 mm
AIII	243 mm
AIV	285 mm

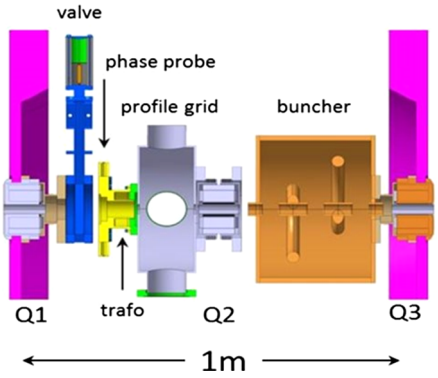

FIG. 2. Intercavity section located between two regular lattice sections.

advances; second, to evaluate this concept in the more general context of quadrupole based lattices with several rf gaps per period. Throughout the paper the stated transverse phase advances refer to the effective sum of transverse focusing by quadrupoles and transverse focusing inside rf gaps. Both signs depend on the quadrupoles polarities and on the signs of the rf phases.

III. PERIODIC LATTICE WITHOUT INTERRUPTIONS

With regard to the more general goal we start in this section with simulations through just the first cavity of the new DTL, referred to as "short lattice," followed by its extension to a "prolonged lattice." For all simulations the TraceWin code has been used [21].

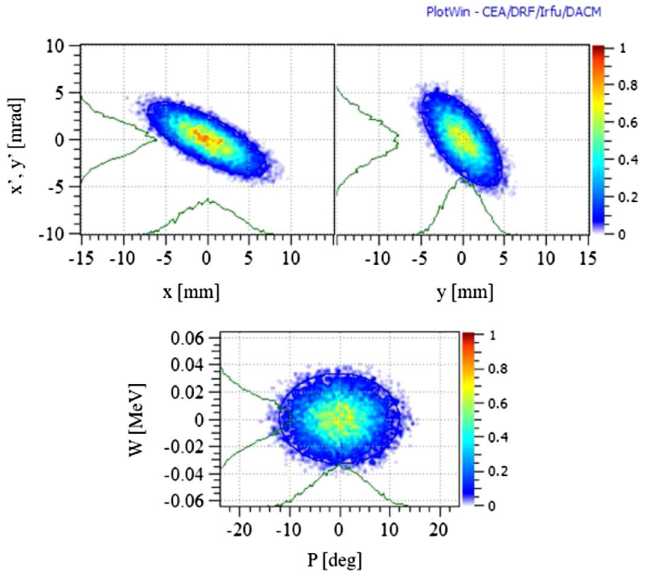

FIG. 3. Distribution at the entrance to the first DTL cavity for a proton beam of 2.0 mA and $k_{0,t} = 50°$, $k_{0,z} = 90°$. The rms emittances are 3.24/3.24/10.8 mm mrad in the horizontal/vertical/longitudinal plane.

A. Short lattice

This case comprises 13.5 complete and strictly periodic DTL lattice periods. The input current is 2.0 mA and acceleration is to 3.3 MeV/u. Figure 3 shows a typical input distribution being a Gaussian cut at 3σ with geometric rms emittances of 3.24/3.24/10.8 mm mrad in the horizontal/vertical/longitudinal plane. This current is space charge equivalent to a $^{238}U^{28+}$ beam of 17 emA, i.e., a relative transverse tune depression of about 35%. To provide for envelope matching, the Twiss parameters β and α in all three planes of freedom have been adapted to each individual setting of $k_{0,t}$ and $k_{0,z}$ [22].

The longitudinal zero current phase advance was scanned in the range from 72° to 145° by changing the rf phase and cavity voltage compared to the original design. The transverse zero current phase advance was independently scanned from 35° to 125°. This two-dimensional scan in the $(k_{0,t}, k_{0,z})$ plane presented in Figs. 4 and 5 quantifies the rms-emittance growth of an accelerated beam in that plane and provides the first test of the only schematic chart in Ref. [12].

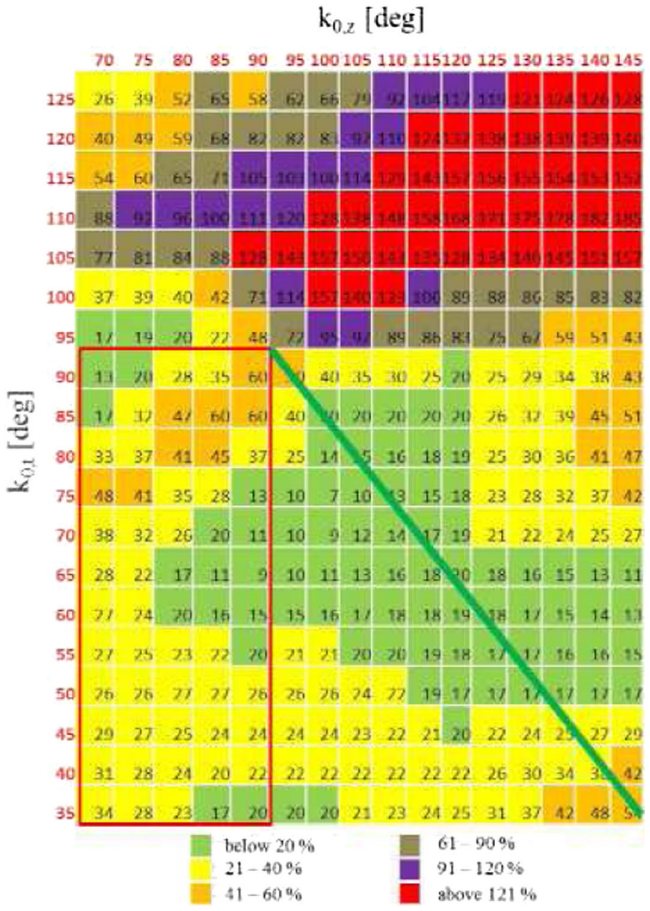

FIG. 4. Relative transverse $(\epsilon_x + \epsilon_y)$ rms-emittance growth for zero current phase advances of $35° \leq k_{0,t} \leq 125°$ and $70° \leq k_{0,z} \leq 145°$ along the first cavity of the DTL for a proton beam of 2.0 mA. The color code corresponding to the growth rates is indicated.

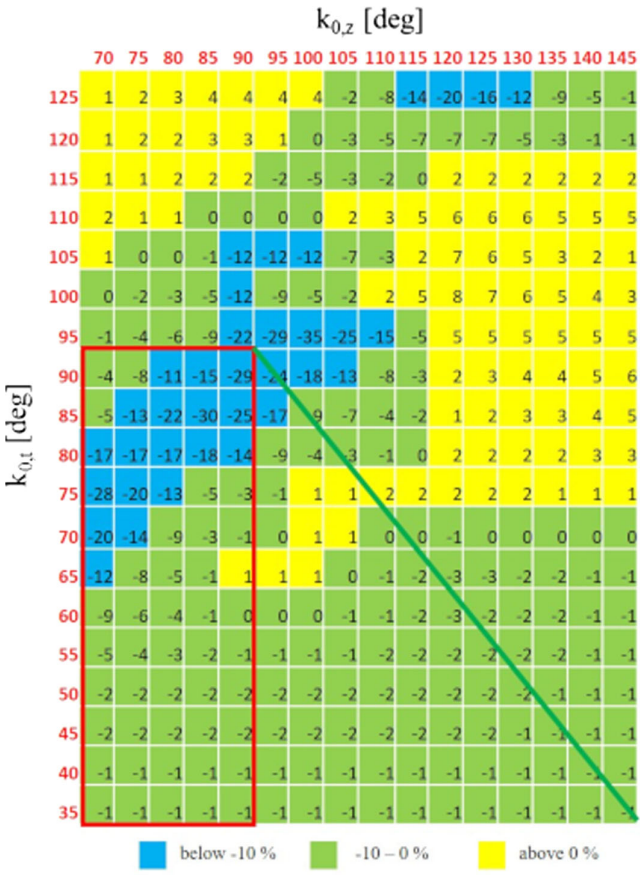

FIG. 5. Relative longitudinal rms-emittance growth for zero current phase advances of $35° \leq k_{0,t} \leq 125°$ and $70° \leq k_{0,z} \leq 145°$ along the first cavity of the DTL for a proton beam of 2.0 mA. Blue cells indicate emittance below −10%, green cells −10%–0%, and yellow cells 0%–10%.

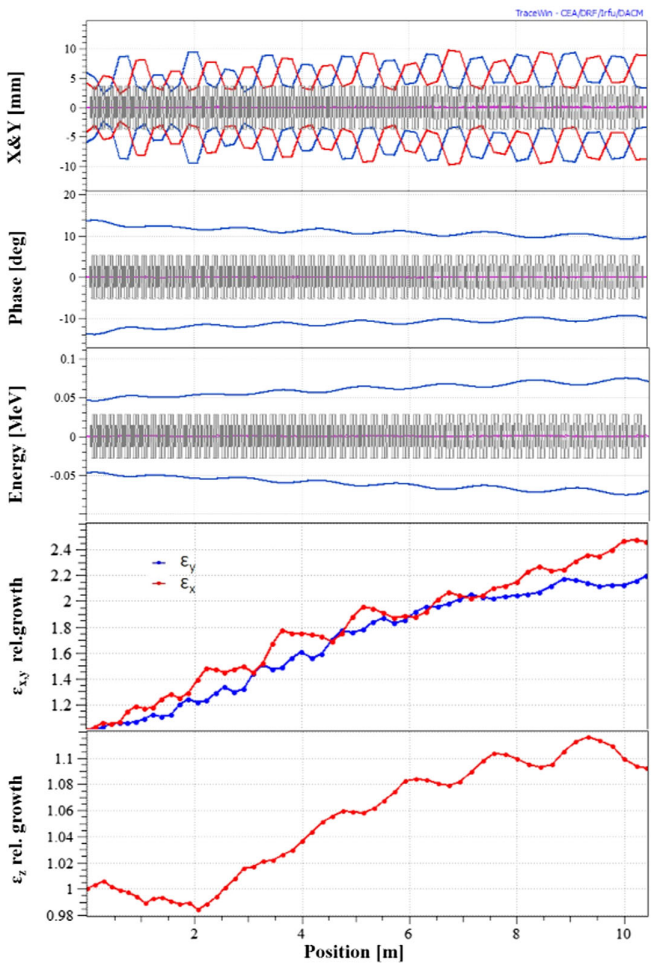

FIG. 6. Beam envelopes, transverse, and longitudinal rms-emittance growth for the unstable case of $k_{0,t} = 110°$, $k_{0,z} = 120°$.

The red framed zone marks the conventional "safe" design rule below 90°. An extended safe region for all values $k_{0,z} > 90°$ is identified as long as $k_{0,t} \leq 90°$. The absence of noticeable emittance growth above the green diagonal line indicates that the theoretically possible sum resonance of Ref. [12] is insignificant for this short lattice. Longitudinal growth shown in Fig. 5 can even be negative, which indicates resonant emittance exchange from the longitudinal to transverse degree of freedom, which was already measured along the existing poststripper at GSI's UNILAC [23]. For the most favorable (green) regions the beam envelopes remain quite periodic and the output distributions have just tiny, negligible halos. In the red regions, instead, the periodicity of beam envelopes is still suitable, but the exit beam qualities are poor and will probably cause beam loss along subsequent cavities (Fig. 6). This agrees with the experimental finding in Ref. [8] that the fourth order resonance dominates, rather than the envelope instability. These findings show that along the short lattice of one single Alvarez-type cavity of 13.5 periods, the longitudinal zero current phase advance of 120° allows to accelerate 2.0 mA of protons with acceptable emittance growth. Moreover, they confirm the existence of an extended design region with longitudinal phase advances well above 90°.

B. Prolonged lattice

In order to provide more general evidence for successful application of $k_{z,0} \geq 90°$ with acceleration, an artificially long DTL cavity comprising 31 DTL periods of FDDF type was constructed from the new DTL design by just merging its cavities AI, AIIa, and AIIb omitting the intercavity sections. The zero current phase advances were fixed to $k_{0,t} = 65°$ and $k_{0,z} = 120°$, with a beam current again 2.0 mA, but acceleration to 7.2 MeV/u. Resulting beam envelopes and rms-emittance growths are presented in Fig. 7. As before, there is again a slight reduction of the longitudinal emittance, while the transverse rms-emittance growth is about 25%. Hence, it was shown that also for very long lattices longitudinal phase advances well above 90° can be applied with tolerable degradation of beam quality. Although the nominal undepressed transverse

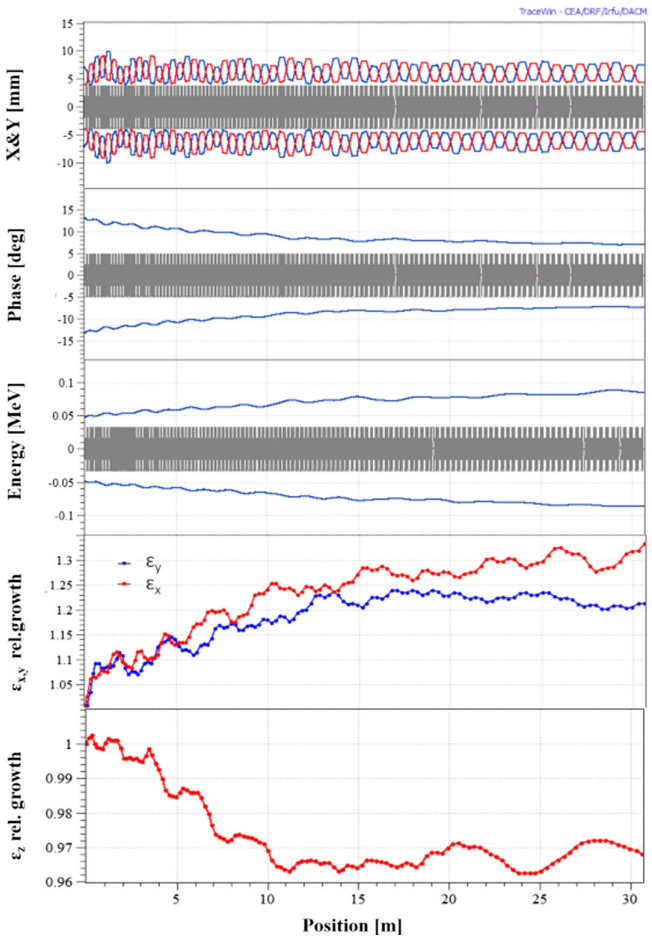

FIG. 7. Beam envelopes, transverse, and longitudinal rms-emittance growth for the prolonged cavity, $k_{0,t} = 65°$, $k_{0,z} = 120°$.

phase advance is 65°, due to finite bunch length some particles experience very low or positive rf phases and hence move partially close to 90° of transverse advance or even beyond. However, these particles comprise just a few percent fraction of the bunch. They are too few to form a coherent space charge driven instability. But they are partially subject to an incoherent particle-core resonance (fourth order resonance). Additionally, these particles have large betatron amplitudes around the rf-bucket center and are less prone to longitudinal depression compared to core particles. For this reason they spend just a fraction of time ($\leq 1/4$) in the above-mentioned regime, i.e., their effective resonant lattice length is shortened such that the time to build up relevant resonance amplitudes is too short. All these effects are included into the simulations as the study aimed at investigating the overall practicability of such operation schemes.

IV. LATTICE WITH INTERCAVITY SECTIONS

In real accelerator lattices the periodicity is interrupted usually several times by inserting intercavity sections

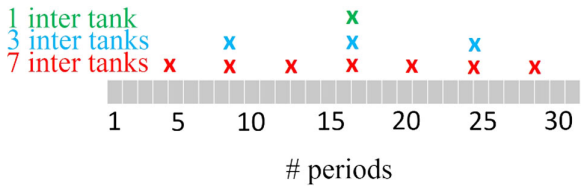

FIG. 8. Sketch of the prolonged beam line comprising 31 complete DTL periods. The locations of intercavity sections for the various scenarios are indicated.

(ICSs) for diagnostics or re-bunchers. To this end the lattice used in Sec. III is interrupted by insertion of several identical ICSs as illustrated in Fig. 8. Three different scenarios were considered, namely (i) one ICS behind DTL period no. 16, (ii) three ICSs behind DTL periods no. 8, no. 16, and no. 24, and (iii) seven ICSs behind DTL periods no. 4, no. 8, no. 12, no. 16, no. 20, no. 24, and no. 28. The three quadrupoles and the rebuncher in each ICS were set to match the beam envelopes between two adjacent cavities. This could be achieved by additional

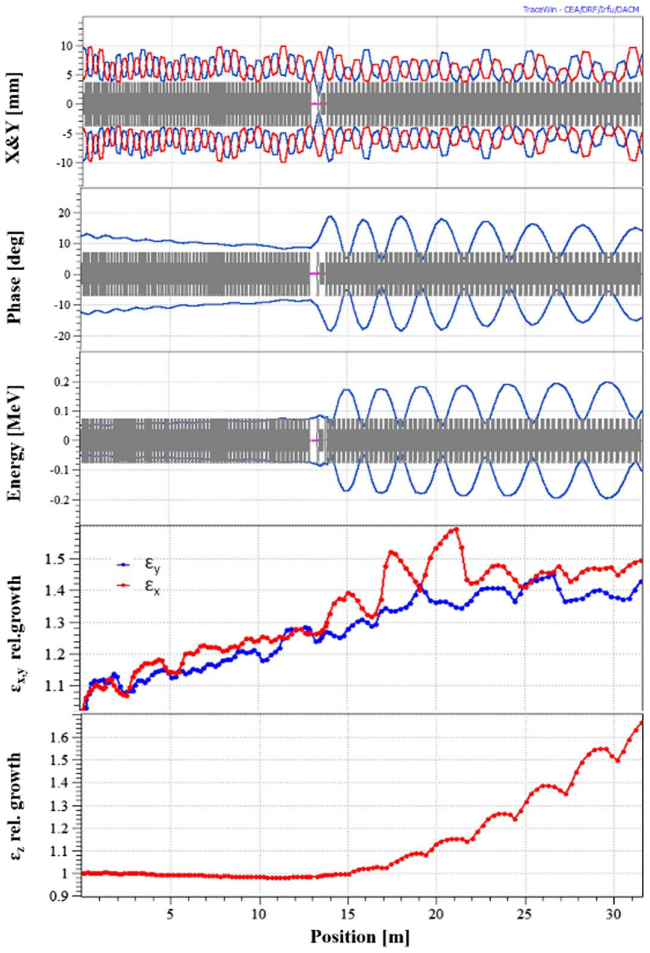

FIG. 9. Beam envelopes, transverse, and longitudinal rms-emittance growth for the prolonged cavity with one intercavity section, $k_{0,t} = 65°$, $k_{0,z} = 120°$.

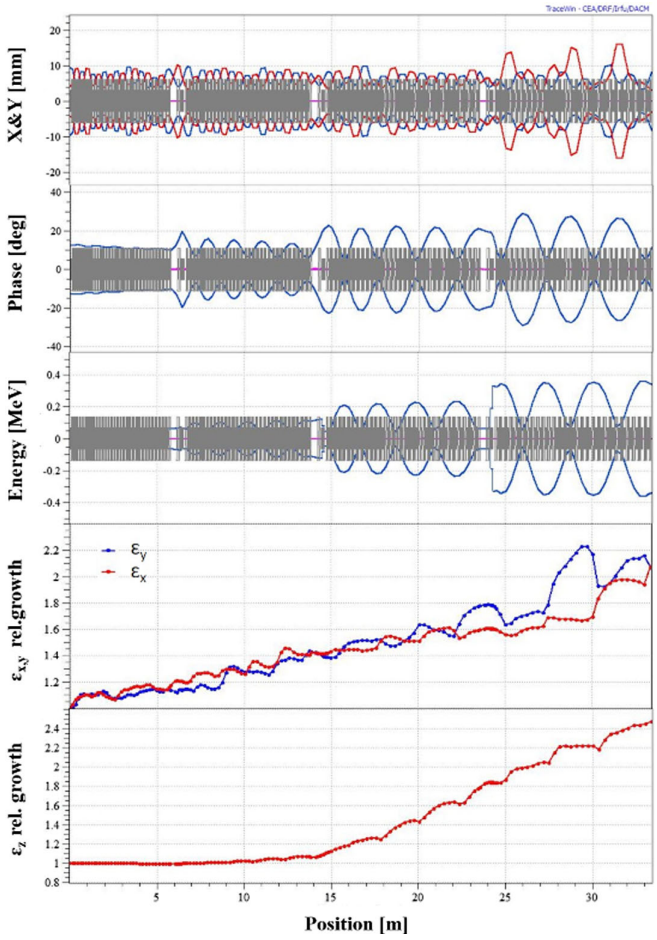

FIG. 10. Beam envelopes, transverse, and longitudinal rms-emittance growth for the prolonged cavity with three intercavity sections, $k_{0,t} = 65°$, $k_{0,z} = 120°$.

slight reduction of the transverse phase advance behind each ICS from the previous 65°. The beam was accelerated without losses, but emittance growth and depressed phase advance variation along the linac are significant, especially for the case with seven ICSs. Figures 9 and 10 depict envelopes, emittance growth, and phase advances of two scenarios, while Table III summarizes the obtained emittance growth for all scenarios.

Hence, the above introduced lattice interruptions considerably harm the beam quality compared to strictly periodic lattices. For the design shown here up to three interruptions of reasonable lengths may be still tolerable,

TABLE III. Rms-emittance growth with several ICSs and $k_{0,t} = 65°$, $k_{0,z} = 120°$.

Number of ICSs	0	1	3	7
Horizontal growth, %	31	71	71	130
Vertical growth, %	20	48	130	580
Longitudinal growth, %	0	71	157	1600

TABLE IV. Rms-emittance growths for the lattice with several intercavity sections (ICSs) and $k_{0,t} = 65°$, $k_{0,z} = 90°$.

Number of ICSs	0	1	3	7
Horizontal growth, %	24	22	75	130
Vertical growth, %	22	30	110	150
Longitudinal growth, %	0	7	8	100

TABLE V. Longitudinal zero current phase advances and corresponding focusing lengths and rf phases applied in the investigations.

$k_{0,l}$ [deg]	φ_{rf} [deg]	L_f [m]
41	−30	9.4
90	−69	2.1
120	−78	1.1

but more of them will definitely not allow for useful beam acceleration. It seems that the required length of interruptions of about one meter is just too long. Up to the rebuncher there is no longitudinal focusing, but rather bunch lengthening. The beam quality degrading effect of this lack of focusing scales with the longitudinal phase advance, which in turn is a measure for the inverse longitudinal focal length. In fact, the longitudinal focusing length at $k_{0,z} = 120°$ is just 1.1 m, which is too close to the length of the interruption of 1.0 m. At $k_{0,z} = 90°$ the longitudinal focusing length is already 2.1 m.

For comparison, an additional investigation of the prolonged lattice with interruptions was done for the case $k_{0,t} = 65°$, $k_{0,z} = 90°$. The results presented in Table IV show much lower emittance growth especially in the longitudinal plane, although the beam quality degradation is still significant. It shall be mentioned that the nominal phase advances applied to the new Alvarez DTL for heavy ion acceleration are $k_{0,t} = 65°$, $k_{0,z} = 41°$, which provide much less emittance growth of just a few percent [16]. In this case the longitudinal focusing length is 9.4 m. Table V summarizes the applied phase advances and the corresponding rf phases and longitudinal focusing lengths.

V. REAL DTL AT 120° LONGITUDINAL PHASE ADVANCE

Finally, the design of the complete new DTL including its ICSs was applied to investigate its capability to accelerate protons to 11.4 MeV/u at longitudinal phase advance of 120°. The design foresees three interruptions of the regular lattice behind the first, third, and fourth cavity [16]. These three interruptions in periodicity, the extremely high longitudinal phase advance of $k_{0,z} = 120°$ and the high beam current of 2.0 mA make the proper beam dynamics design a nontrivial task. Proper matching makes the beam passing the DTL without losses; however the resulting

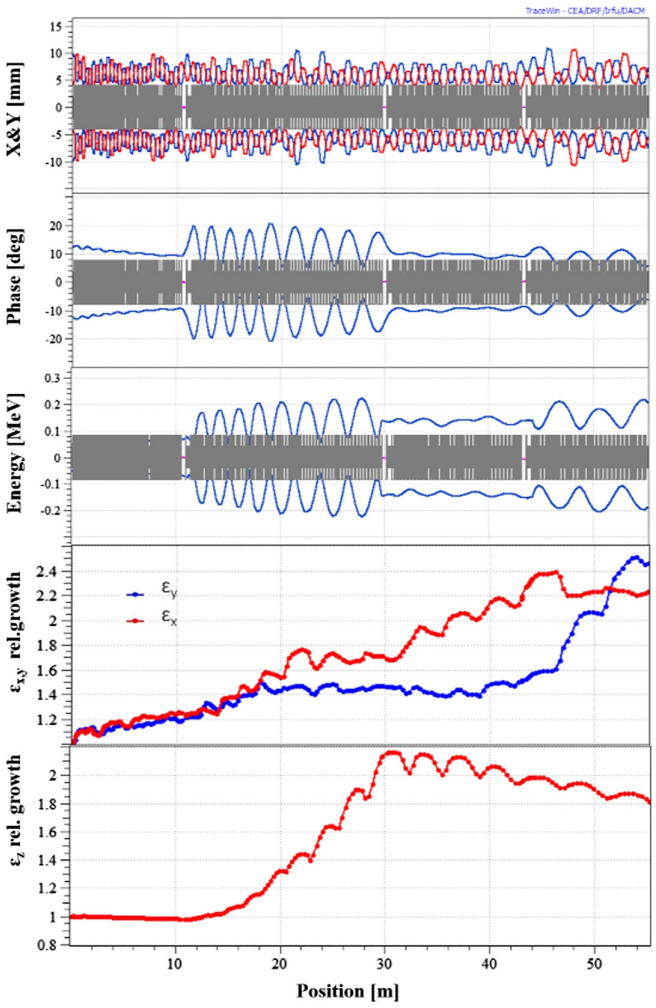

FIG. 11. Beam envelopes, transverse, and longitudinal rms-emittance growth for the complete DTL with intercavity sections and $k_{0,t} = 65°$, $k_{0,z} = 120°$.

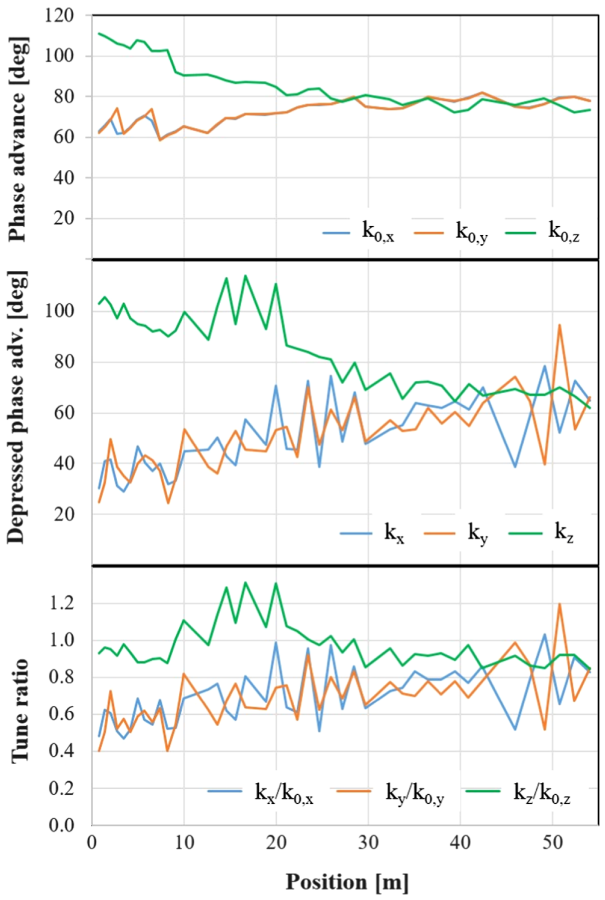

FIG. 12. Zero current phase advance, depressed phase advance, and tune depression for the complete DTL with intercavity sections and $k_{0,t} = 65°$, $k_{0,z} = 120°$.

130% transverse emittance growth is significant. Figure 11 plots the corresponding envelopes and growth rates along the DTL. The variation of depressed phase advance is large along the second and third cavity (Fig. 12) as a consequence of reasonable matching to the last two cavities.

Depressed phase advances are determined from the dynamics of the simulated distribution. This method is prone to noise from large amplitude particles especially for large envelope breathing of the beam (mismatched beam). Local positive fluctuations of the depressed longitudinal phase advance suggest negative depressions. These occur along the part of the lattice where the longitudinal matching is not good (compare to phase and energy amplitudes shown in Fig. 11). Longitudinal intercavity matching is accomplished by just one rebuncher amplitude, hence too few parameters, and partially poor matching is achieved at high longitudinal phase advances. We argue that the method of depressed phase advance determination together with the local mismatch leads to the suggested local negative longitudinal depression.

The simulated emittance growth seems high, but has to be judged considering that the DTL's design is dedicated to provision of heavy ions with 8 times higher rigidity and corresponding emittance growth of just a few percent [16]. In summary, operation at longitudinal phase advance of 120°, i.e., well above 90°, is feasible. The observed beam quality degradation is not related to the resonant processes at the 90° stop band. Instead, it is due to the requirement of intercavity sections interrupting the lattice periodicity and generating mismatch.

VI. CONCLUSIONS

The proposal of extending the range of longitudinal phase advances beyond 90° has been applied to proton acceleration in the design lattice of a real DTL to be built and under prototyping at GSI. An idealized strictly periodic prolongation of the lattice of the first cavity is found to confirm acceleration at 120° with practically no resonance effect on emittances.

However, interrupting the periodicity by extended intercavity sections—indispensable for accelerating a broad spectrum of ions—deteriorates the final quality of the

proton beam. This is not related to resonance effects, but a consequence of insufficient matching to maintain periodic envelopes across interruptions. For $k_{0,z} = 120°$ per lattice period the overall deterioration is still acceptable if only three intercavity sections are used.

We conclude that the feasibility of accelerating above 90° of longitudinal phase advance has been demonstrated for a lattice with more than a single rf gap per structure period. Besides the example studied here, the additional design freedom may warrant similar studies for superconducting linear accelerator lattices. In case of quadrupolar focusing, for example, where the rf period is a fraction of the lattice focusing period, stronger longitudinal focusing not limited to below 90° may allow more efficient use of the superconducting rf with possibly cost saving effects. As shown here, matching challenges between tanks grow with increasing $k_{0,z}$, which requires similar careful studies.

[1] T. P. Wangler, *RF Linear Accelerators, Second Edition* (Wiley-VCH, New York, 2008).

[2] Z. H. Li, F. Yan, J. Y. Tang, H. P. Geng, C. Meng, P. Cheng, B. Sun, and Z. Guo, Beam dynamics of China ADS linac, in *Proceedings of the 52nd ICFA Beam Dynamics Workshop, Beijing, People's Republic of China*, edited by N. Zhao (IHEB, Beijing, 2012).

[3] J.-F. Ostiguyy, A. Saini, N. Solyak, J.-P. Carneiro, and V. Lebedev, Lattice design and beam dynamics studies for Project X, in *Proceedings of the XXVI Linear Accelerator Conference, Tel-Aviv, Israel*, edited by M. Draper (CERN, Geneva, 2013).

[4] L. Zhi-Hui and T. Jing-Yu, A cw superconducting linac as the proton driver for a medium baseline neutrino beam in China, Chin. Phys. C **38**, 12 (2014).

[5] I. Hofmann *et al.*, Stability of the K-V distribution in long periodic transport systems, Part. Accel. **13**, 145 (1983).

[6] J. Struckmeier and M. Reiser, Theoretical studies of envelope oscillations and instabilities of mismatched intense charged-particle beam in periodic focusing channel, Part. Accel. **14**, 227 (1984).

[7] M. G. Tiefenback and D. Keefe, Measurements of stability limits for a space-charge-dominated ion beam in a long a. G. transport channel, IEEE Trans. Nucl. Sci. **32**, 2483 (1985).

[8] L. Groening, W. Barth, W. Bayer, G. Clemente, L. Dahl, P. Forck, P. Gerhard, I. Hofmann, M. S. Kaiser, M. Maier, S. Mickat, T. Milosic, D. Jeon, and D. Uriot, Experimental Evidence of the 90° Stop Band in the GSI UNILAC, Phys. Rev. Lett. **102**, 234801 (2009).

[9] D. Jeon, L. Groening, and G. Franchetti, Fourth order resonance of a high intensity linear accelerator, Phys. Rev. ST Accel. Beams **12**, 054204 (2009).

[10] C. Li and Y. L. Zhao, Envelope instability and the fourth order resonance, Phys. Rev. ST Accel. Beams **17**, 124202 (2014).

[11] I. Hofmann and O. Boine-Frankenheim, Space-Charge Structural Instabilities and Resonances in High-Intensity Beam, Phys. Rev. Lett. **115**, 204802 (2015).

[12] I. Hofmann and O. Boine-Frankenheim, Revisiting the Longitudinal 90° Limit in High Intensity Linear Accelerators, Phys. Rev. Lett. **118**, 114803 (2017).

[13] J. Qiang, Three-dimensional envelope instability in periodic focusing channels, Phys. Rev. Accel. Beams **21**, 034201 (2018).

[14] O. Boine-Frankenheim, I. Hofmann, and J. Struckmeier, Parametric sum envelope instability of periodically focused intense beams, Phys. Plasmas **23**, 090705 (2016).

[15] Y. Yuan, O. Boine-Frankenheim, and I. Hofmann, Modeling of second order space charge driven coherent sum and difference instabilities, Phys. Rev. Accel. Beams **20**, 104201 (2017).

[16] S. Mickat *et al.*, *Concept towards a new Alvarez-type poststripper DTL for the UNILAC* (GSI, Darmstadt, 2017).

[17] S. Mickat, X. Du, P. Gerhard, L. Groening, M. Heilmann, M. Kaiser, A. Rubin, V. Srinivasan, and W. Sturm, Layout of the new FAIR poststripper DTL for intense heavy ion beams, in *Proceedings of the XXVIX Linear Accelerator Conference, Beijing, People's Republic of China*, edited by G. Pei (IHEP, Beijing, 2018).

[18] P. Spiller and G. Franchetti, The FAIR accelerator project at GSI, Nucl. Instrum. Methods Phys. Res., Sect. A **561**, 305 (2006).

[19] A. Rubin, X. Du, L. Groening, M. S. Kaiser, and S. Mickat, Status of the beam dynamics design of the new poststripper DTL for GSI–FAIR, in *Proceedings of the 17th International Particle Accelerator Conference, Copenhagen, Denmark*, edited by G. Arduini (Geneva, Switzerland, 2017).

[20] C. Xiao, A. Rubin, and L. Groening, Stable beam operation of drift tube linac cavities at voltages far below design, Nucl. Instrum. Methods Phys. Res., Sect. A **928**, 70 (2019).

[21] http://irfu.cea.fr/dacm/logiciels/index.php.

[22] L. Groening, W. Barth, W. Bayer, G. Clemente, L. Dahl, P. Forck, P. Gerhard, I. Hofmann, G. Riehl, and S. Yaramyshev, Benchmarking of measurement and simulation of transverse rms-emittance growth, Phys. Rev. ST Accel. Beams **11**, 094201 (2008).

[23] L. Groening, I. Hofmann, W. Barth, W. Bayer, G. Clemente, L. Dahl, P. Forck, P. Gerhard, M. S. Kaiser, M. Maier, S. Mickat, T. Milosic, and S. Yaramishev, Experimental Evidence of Space Charge Driven Emittance Coupling in High Intensity Linear Accelerators, Phys. Rev. Lett. **103**, 224801 (2009).